LRPPRC confers enhanced oxidative phosphorylation metabolism in triple-negative breast cancer and represents a therapeutic target

Qiqi Xue[1,2,3†], Wenxi Wang[1,2†], Jie Liu[2], Dachi Wang[2], Tianyu Zhang[1,2], Tingting Shen[2], Xiangsheng Liu[2], Xiaojia Wang[2,4], Xiying Shao[4*], Wei Zhou[2*] and Xiaohong Fang[1,2,3*]

Abstract

Background Triple-negative breast cancer (TNBC) is a highly malignant tumor that requires effective therapeutic targets and drugs. Oxidative phosphorylation (OXPHOS) is a metabolic vulnerability of TNBC, but the molecular mechanism responsible for the enhanced OXPHOS remains unclear. The current strategies that target the electronic transfer function of OXPHOS cannot distinguish tumor cells from normal cells. Investigating the mechanism underlying OXPHOS regulation and developing corresponding therapy strategies for TNBC is of great significance.

Methods Immunohistochemistry and sequencing data reanalysis were used to investigate LRPPRC expression in TNBC. In vitro and in vivo assays were applied to investigate the roles of LRPPRC in TNBC progression. RT-qPCR, immunoblotting, and Seahorse XF assay were used to examine LRPPRC's functions in the expression of OXPHOS subunits and energy metabolism. In vitro and in vivo functional assays were used to test the therapeutic effect of gossypol acetate (GAA), a traditional gynecological drug, on LRPPRC suppression and OXPOHS inhibition.

Results LRPPRC was specifically overexpressed in TNBC. LRPPRC knockdown suppressed the proliferation, metastasis, and tumor formation of TNBC cells. LRPPRC enhanced OXPHOS metabolism by increasing the expression of OXPHOS complex subunits encoded by the mitochondrial genome. GAA inhibited OXPHOS metabolism by directly binding LRPPRC, causing LRPPRC degradation, and downregulating the expression of OXPHOS complex subunits encoded by the mitochondrial genome. GAA administration suppressed TNBC cell proliferation, metastasis in vitro, and tumor formation in vivo.

Conclusions This work demonstrated a new regulatory pathway of TNBC to promote the expression of mitochondrial genes by upregulating the nuclear gene *LRPPRC*, resulting in increased OXPHOS. We also suggested

†Qiqi Xue and Wenxi Wang contributed equally to this work.

*Correspondence:
Xiying Shao
shaoxy@zjcc.org.cn
Wei Zhou
zhouwei@him.cas.cn
Xiaohong Fang
xfang@iccas.ac.cn
Full list of author information is available at the end of the article

Xue *et al. Journal of Translational Medicine*   (2025) 23:372

Page 2 of 15

a promising therapeutic target LRPPRC for TNBC, and its inhibitor, the traditional gynecological medicine GAA, presented significant antitumor activity.

Keywords Triple-negative breast cancer, Gossypol acetate, Oxidative phosphorylation

Introduction

Breast cancer has surpassed lung cancer as the most frequently diagnosed malignant tumor, with around 2.3 million new cases each year, leading to 685 thousand deaths [1]. Molecular typing based on multi-omics categorizes breast cancer into three subtypes: luminal, epidermal growth factor receptor-2 (HER2) overexpression, and basal-like [2]. The basal-like subtype, also known as triple-negative breast cancer (TNBC), is the most aggressive form of breast cancer and accounts for about 15%–20% of breast cancer cases [3]. Nearly 46% of TNBC patients experience distant metastasis [4], with a median survival time of only 13.3 months after metastasis [5]. As TNBC shows negative in estrogen receptor (ER), progesterone receptor (PR), and HER2 expression, it does not respond to current endocrine therapy or anti-HER2 targeted therapy [5]. Currently, the main treatments for TNBC are chemotherapy and radiotherapy, which are limited in efficacy and have significant side effects [5]. Therefore, it is crucial to explore the vulnerabilities of TNBC to develop new targeted therapeutic approaches.

The majority of TNBC patients harbor inactivated tumor suppressor RB Transcriptional Corepressor 1 (RB1, mutation or copy number deletion) [6]. The inactivation of RB1 confers TNBC the ability to grow rapidly independent of extracellular growth signal and the CDK4/6 kininase activity, indicating TNBC is unlikely to benefit from the growth factor receptor inhibitors or the latest CDK4/6 inhibitors [7]. TNBC cells harbor a robust OXPHOS function, which endows them with a fast growth rate, chemotherapy tolerance, and a high proportion of tumor stem cells [7]. Pre-clinical researches have confirmed the inhibition of OXPHOS represents a promising strategy for some TNBC [8]. However, there are unsolved concerns about the clinical application of OXPHOS inhibitors. The most significant issue is the molecular mechanism behind the enhanced OXPHOS in TNBC remains elusive. The OXPHOS complex is encoded by both nuclear and mitochondrial DNA. Although a few studies explain in part the mechanism underlying the upregulation of OXPHOS protein subunits encoded by nuclear genes in TNBC [9], little is known regarding the regulation of the expression of OXPHOS subunits encoded by mitochondrial genome. The absence of this information impedes our ability to efficiently screen TNBC—responsive OXPHOS inhibitors. In addition, current OXPHOS-targeting therapies (metformin, oligomycin, rotenone, etc.) concentrate primarily on directly inhibiting the activity of OXPHOS complexes, which makes it impossible to differentiate between normal cells and tumor cells, resulting in deleterious side effects. Therefore, it is imperative to develop new OXPHOS-inhibiting strategies with improved anti-cancer efficacy and minimal adverse effects.

Leucine Rich Pentatricopeptide Repeat Containing (LRPPRC) is an RNA-binding protein that binds to all 13 mitochondrial gene-encoded mRNAs of the OXPHOS complex and improves their mRNA stability and translation efficacy [10–12]. In this study, we identified LRPPRC as a biomarker of tumor progression and therapeutics for TNBC. In breast cancer, LRPPRC is specifically overexpressed in TNBC, at both RNA level and protein level. Knockdown of LRPPRC significantly inhibited the malignant phenotypes of TNBC cells in vitro and in vivo. Mechanically, TNBC upregulates the expression of LRPPRC protein by the abnormal DNA methylation at the promoter of the LRPPRC gene and universal DNA copy amplification. Enhanced LRPPRC level upregulates the expression of OXPHOS subunits encoded by mitochondrial genes, thereby enhancing cellular OXPHOS metabolism to support tumor cell proliferation and metastasis. Importantly, the widely used gynecological drug gossypol acetate (GAA) binds directly to LRPPRC and induces its degradation [13–15]. GAA induces synthetic defects in OXPHOS subunits, as opposed to conventional OXPHOS-suppression strategies that inhibit the activity of existing OXPHOS complexes [13]. GAA inhibits the OXPHOS metabolism of TNBC and exhibits significant antitumor activity in vitro and in vivo. Overall, we have demonstrated a new molecular mechanism for the enhanced OXPHOS metabolism in TNBC and devised a targeted intervention strategy that provides a valuable direction for the targeted treatment of TNBC.

Methods

Public database analysis

Survival analyses (Fig. 1E, F) were conducted with the online tool KM Plotter (https://kmplot.com/analysis/). LRPPRC protein level analyses in different breast cancer subtypes (Fig. 1B) were conducted on online analysis website UALCAN (http://ualcan.path.uab.edu/

Xue *et al. Journal of Translational Medicine*   (2025) 23:372
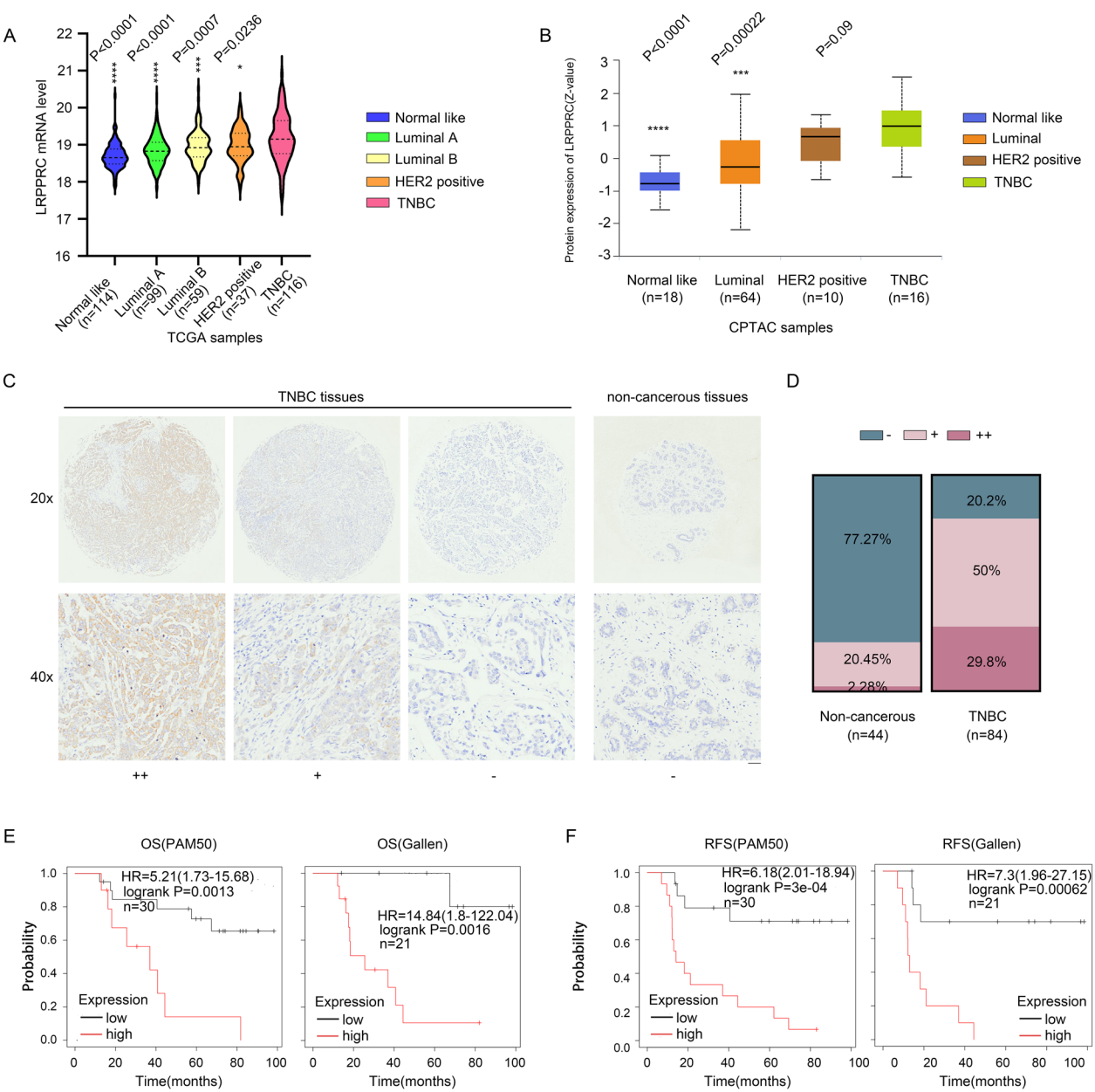
Page 3 of 15

Fig. 1 LRPPRC is upregulated in TNBC tissues and related to a worse prognosis. **A** LRPPRC mRNA levels were correlated with subtype in the TCGA breast cancer dataset. Student *t*-test was performed to compare TNBC with other subtypes of breast cancer. **B** LRPPRC expression levels were correlated with subtype in the CPTAC breast cancer dataset. Student *t*-test was performed to compare TNBC with other subtypes of breast cancer. **C** Representative IHC images of non-cancerous tissues (n = 44) and TNBC tissues (n = 84) stained by hematoxylin and eosin (H&E) and with LRPPRC antibody. Staining intensity of LRPPRC in TNBC tissues is classified as negative staining (−), weak staining (+), and strong staining (+ +). The scale bar is 50 pixels. **D** Percentage of negative staining, weak staining, and strong staining samples in TNBC tissues and non-cancerous tissues with LRPPRC antibody. **E, F** Kaplan–Meier survival analysis of association of LRPPRC expression with overall survival (OS) and recurrence-free survival (RFS) of patients in the clinical dataset GSE42568. *$P < 0.05$. **$P < 0.01$. ***$P < 0.001$. ****$P < 0.0001$

index.html) [16, 17]. The RNA expression and DNA methylation data about LRPPRC in normal tissues and different subtypes of breast cancer (Figs. 1A, 2A–C) were downloaded from the online analysis website

MEXPRESS [18, 19]. The omics data for each cancer in the MEXPRESS have integrated all datasets from TCGA, and specific dataset information is no longer displayed here. The analyses of the correlation between DNA copy number and LRPPRC expression level
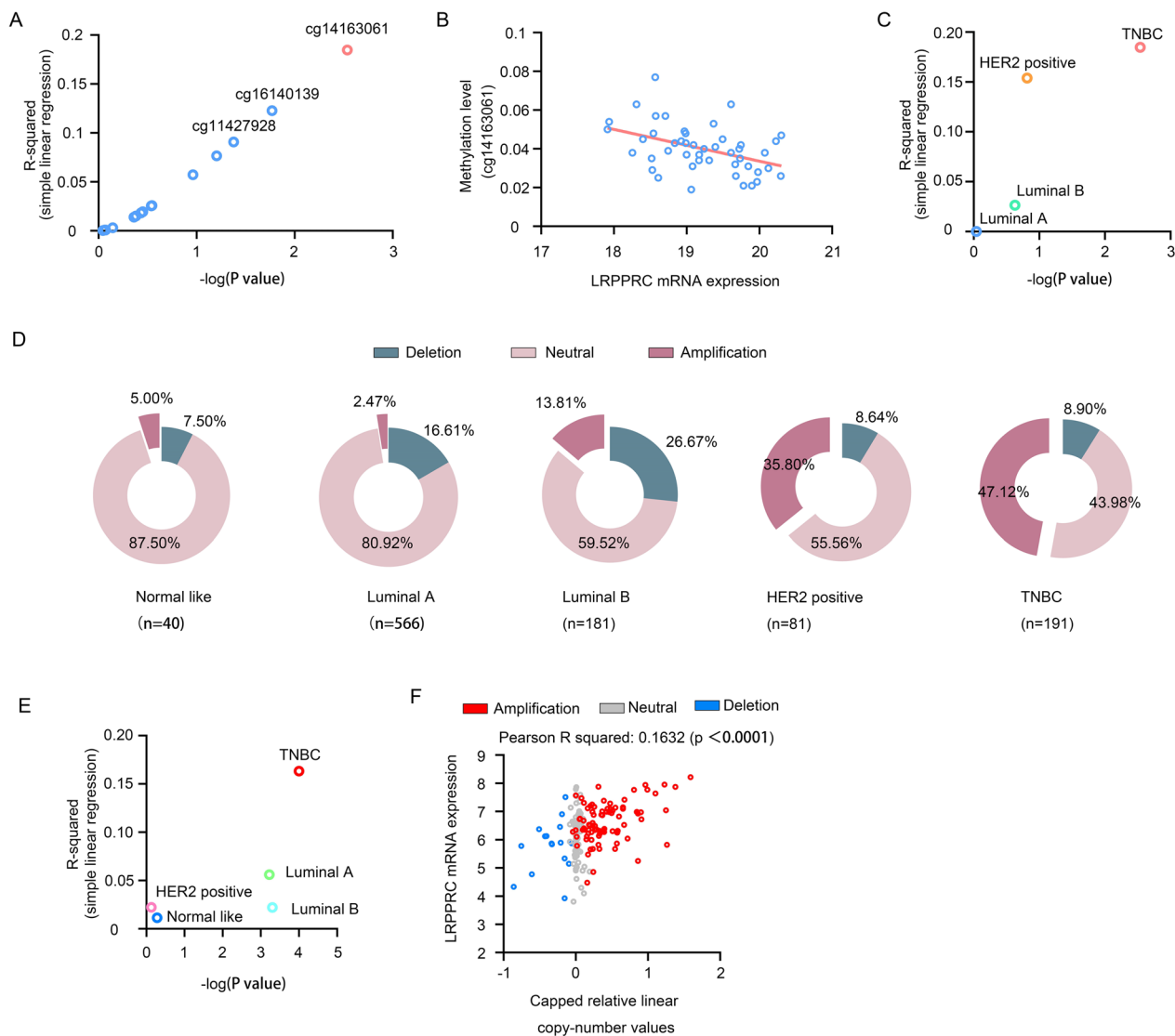
Xue *et al. Journal of Translational Medicine*　　(2025) 23:372

Page 4 of 15

Fig. 2 DNA methylation level and copy number are related to LRPPRC overexpression in TNBC. **A** Correlation analysis of LRPPRC gene methylation status at each CpG site and LRPPRC mRNA expression level in TNBC samples provided by the TCGA dataset. Simple linear regression test was used. **B** Correlation analysis of LRPPRC gene methylation status at cg14163061 and LRPPRC mRNA expression in TNBC samples provided by the TCGA dataset. Simple linear regression test was used. **C** Correlation analysis of LRPPRC gene methylation status at cg14163061 and LRPPRC mRNA expression level in different breast cancer subtypes. Simple linear regression test was used. **D** Frequency of LRPPRC copy number variation of different breast cancer subtypes in the TCGA, hg19 was used as the reference genome. **E** Correlation analysis of LRPPRC copy number variation with LRPPRC mRNA expression level of different breast cancer subtypes in the TCGA breast cancer dataset. Simple linear regression test was used. **F** Correlation analysis of LRPPRC copy number variation and mRNA expression level of TNBC in the TCGA breast cancer dataset. Simple linear regression test was used

(Fig. 2D–F) were conducted using all the breast cancer sequence data collected in TCGA.

Cell culture
SUM-159 and MDA-MB-468 cell lines were obtained from the American Type Culture Collection (ATCC, Manassas, VA, United States). SUM-159 cells were grown in RPMI 1640 (Gibco, Waltham, MA, United States) containing 10% FBS (Gibco) under aseptic conditions and incubated at 37 ℃ with 5% CO_2. MDA-MB-468 cells were maintained in Leibovitz's L-15 (Dalian meilun Biotechnology, Dalian, China) containing 10% FBS under aseptic conditions and incubated at 37℃ with 0.1% CO_2.

Xue *et al. Journal of Translational Medicine*   (2025) 23:372

Page 5 of 15

LRPPRC stable knockdown

To generate LRPPRC stable knockdown cells, lentivirus containing LRPPRC-specific shRNA was purchased from Genechem Company (Shanghai, China). Cells were transfected with diluted lentivirus for 48 h, and then the puromycin-containing medium was added to select the successfully infected cells. The information of shRNA sequences: sh-LRPPRC-1: CCTCAAAGGAATGCAAGAATT; sh-LRPPRC-2: GGAGGAGCATTTGAGACAATA.

Cell proliferation assay

TNBC control and gene knocked-down cells (2000 cells per well) were seeded in an E-plate and transferred to an RTCA analysis system that was maintained at 37 ℃. To generate the growth curves, the cell index of each well was monitored every 1 h using RTCA software with an integrated confluence algorithm until 80–124 h.

Clonogenic assay

500–1000 cells were seeded in 12-well plates and treated with different concentrations of GAA for 48 h. Cells were washed twice with a complete medium and further cultured in an incubator at 37 ℃. At the indicated time point (usually 10–14 days), cells were fixed with 80% methanol and stained with crystal violet solution overnight. All experiments were performed in triplicate.

Transwell assay

Migration and invasion assays were performed using chambers with a diameter of 6.5 mm and pore size of 8.0 μm according to the instructions of the manufacturer (Corning, America). Briefly, 2×10^5 cells were plated in serum-free medium in the upper chamber with a non-coated membrane for the migration assay and with a Matrigel-coated membrane for the invasion assay. The lower chamber was filled with a medium containing 10% serum. Then, the cells on the upper surface were removed by cotton swab and the cells on the lower surface were stained with crystal violet and observed under a microscope.

Western blot analysis

Cells were lysed in RIPA lysis buffer (#C1053-100, Applygen, China), containing protease inhibitor cocktail (#P1266-1, Applygen, China), and phosphatase inhibitors (#P1260-1, Applygen, China). Equal amounts of protein (30–60 μg) were separated by 10% SDS–PAGE and transferred to the PVDF membrane (#03010040001, MERCK, America) for further processing, following standard western blotting procedures. The primary antibodies were diluted with BSA using the following concentrations: Anti-GAPDH (Cell Signaling Technology, #97166, 1:5000), Anti-LRPPRC (Santa Cruz Biotechnology, #sc-166178, 1:2000), Anti-total OXPHOS antibody cocktail (Abcam, ab110413, 1:2000 or Proteintech, PK30006, 1:2000). After thorough washing, the HRP-labeled secondary antibody (PROMEGA, W401B, 1:3000; W402B, 1:2000) was added for 1 h at room temperature. The protein luminescence signal was acquired using the Amersham ImageQuant 800 (GE, America) and ImageJ was used to quantify western blotting results by densitometry.

RNA isolation, cDNA synthesis, and Real Time Quantitative PCR

Total RNA was isolated from cells by using the QIAamp RNA Mini Kit (50) (QIAGEN) following the manufacturer's instructions. 2 μg of total RNA was subjected to first-strand cDNA synthesis by using the Hifair II 1st Strand cDNA Synthesis Kit (YEASEN, 11121ES60). Briefly, DNase is used to remove residual genomic DNA at 42 ℃. Then, reverse transcriptase and random primers were added to synthesize cDNA at 55 ℃. RT-PCR was performed in a 20μL reaction volume according to the manufacturer's protocol via SYBR Premix Ex Taq (YEASEN, 11199ES03), in a white 96-multiwell plate by using an CFX96 Real-Time PCR system (Applied Biosystems, California, USA). To quantify the data, the comparative Ct method was used. Relative quantity was defined as log2ΔΔCt and GAPDH was used as a reference gene. The sequence of PCR primers was listed in supplemental table S1.

Metabolic phenotypes

For the OCR assay, SUM-159 and MDA-MB-468 cells were suspended at a concentration of 4×10^5 cells/mL. 100 μL of cells were added to Seahorse 24-well plates. After adhering to the wall, the cells were treated with gradient concentrations of GAA in 500 μL complete medium for 48 h. Then the medium was discarded, and the cells were washed with 500 μL pre-warmed Seahorse medium (Seahorse XF medium with 2 mM glutamate, 10 mM glucose, and 2 mM pyruvate). Basal oxygen consumption was determined in the Seahorse medium. Oligomycin was added to determine the oxidative leak, and carbonyl cyanide m-chlorophenyl (CCCP) was added to stimulate the mitochondrial electron transport chain to the max. Finally, rotenone and antimycin A were added to measure extra-mitochondrial respiration.

Animal experiments

Female mice aged 4 weeks were purchased from Hangzhou Medical College Laboratory Animal Centre, Zhejiang Center of Laboratory Animals, and reared under specific pathogen-free conditions. All the mice-related studies were approved by The Cancer Hospital of

Xue *et al. Journal of Translational Medicine*   (2025) 23:372

Page 6 of 15

the University of Chinese Academy of Sciences. All mice were treated humanely throughout the experimental period. To evaluate the roles of LRPPRC in tumorigenesis in vivo, SUM-159 control cells or LRPPRC knockout cells were injected into nude mice subcutaneously. The tumor volumes were measured every 5 days using digital calipers, and volumes were calculated as (length $\times$ width^2)/2. To evaluate the anti-tumor effect of GAA, SUM-159 cells were injected subcutan eously to establish a TNBC tumor model. When the tumor volume reached about 100 mm^3, mice were randomly divided into experimental and control groups. GAA-loaded MSNPs were dissolved in PBS to a final concentration of 2.4 mg/mL, and each mouse received a dose of 150 µL by tail vein injection every three days. The mice were sacrificed to strip the subcutaneous tumors. Then the xenograft tumors were fixed with 10% formalin, embedded by paraffin, and cut into 5 µm-thick sections for immunohistochemical analysis. The humane endpoint for tumor size was 1500 mm^3.

Statistical analysis

Data were given as mean $\pm$ s.e.m. Details of the number of biological replicates were given in the figure legends. Statistical analysis was performed using GraphPad Prism version 8.0. Student t-test, One-Way ANOVA, or Two-way ANOVA was used for comparison between control groups and experimental groups. *NS*, not significantly; *$P < 0.05$; **$P < 0.01$; ***$P < 0.001$. ****$P < 0.0001$.

Results

LRPPRC is a specific tumor biomarker overexpressed in TNBC

Preclinical studies have shown that OXPHOS is a viable therapeutic target for TNBC[8]. LRPPRC is one of the most essential regulators of OXPHOS and our previous works have demonstrated that it is a novel lung cancer progression marker and therapeutic target[13]. To test the roles of LRPPRC in TNBC, we first reanalyzed the RNA and protein expression data in public databases, including the Cancer Genome Atlas Program (TCGA) and Clinical Proteomic Tumor Analysis Consortium (CPTAC). The mRNA sequencing data from the TCGA database revealed that LRPPRC mRNA levels in TNBC were significantly higher than that in all breast cancer subtypes (TNBC versus Luminal A subtype patients, $P < 0.0001$; TNBC versus Luminal B subtype patients, $P = 0.0007$;TNBC versus HER2 positive subtype, $P = 0.0236$, Fig. 1A). We also analyzed TNBC proteomic data from the CPTAC database. TNBC expressed a higher level of LRPPRC protein than other subtypes of breast cancer (TNBC versus normal like tissues, $P < 0.0001$; TNBC versus Luminal subtype, $P = 0.00022$;

TNBC versus HER2 positive subtype, $P = 0.09$, Fig. 1B), consistent with the above-mentioned patterns of mRNA data. We then verified the overexpression of LRPPRC in TNBC samples (n $= 84$, one tissue sample per individual) and non-cancerous samples (n $= 44$, one tissue sample per individual) using immunohistochemistry in tissue array. 79.8% of TNBC samples were LRPPRC positive (28.9% high expression and 50% medium expression), which was significantly higher than that in non-cancerous tissues (2.28% high expression and 20.4% medium expression) (Fig. 1C, D). Furthermore, in a separate group of individuals in the clinical dataset GSE42568, the 5-year overall survival (OS) and recurrence-free survival (RFS) of the LRPPRC high expression group were significantly poorer than those of the LRPPRC low expression group (Fig. 1E, F). These results indicated that the expression of LRPPRC was specifically increased in TNBC and highly correlated with poor prognosis of patients.

LRPPRC is regulated by DNA methylation and DNA copy number variation in TNBC

Next, we explored the potential factors responsible for the specific enhanced expression of LRPPRC in TNBC. There are 15 DNA methylation sites around the LRPPRC gene, and the level of methylation at these specific locations can potentially impact the expression of LRPPRC (Supplemental file1: FigureS1 A). The methylation degrees of three sites were significantly correlated with mRNA level of LRPPRC in TNBC ($P < 0.05$), two of which located in its promoter (Fig. 2A and Supplemental file1: Fig. S1 A). Ultimately, we assessed the correlation between the methylation levels of these two sites and the mRNA expression of LRPPRC across various breast cancer subtypes. Notably, only the negative correlation between cg14163061 methylation and LRPPRC expression was confined to TNBC, with no such correlation observed in cg01913188 site (Fig. 2B, C and Supplemental file1: Figure S1 B). Therefore, we proposed cg14163061 might be the major methylation site contributing to the specific high expression of LRPPRC protein in TNBC.

We also examined the impact of gene copy number variation on the expression of LRPPRC in TNBC. We integrated all breast cancer DNA sequencing data on TCGA, and quantified the copy number of LRPRPC in online analysis website Cbioportal (https://www.cbiop ortal.org/), using the latest hg19 as the reference genome. DNA copy number analysis from the TCGA breast cancer dataset showed that the copy number of LRPPRC in TNBC was elevated (Fig. 2D). In addition, the copy number amplification percentage of LRPRPC in TNBC was also higher than other subtypes of breast cancer (Fig. 2D). More specifically, 47.12% of TNBC samples

Xue *et al. Journal of Translational Medicine*   (2025) 23:372

Page 7 of 15

exhibited an elevated DNA copy number of LRPPRC gene, surpassing the percentages observed in the normal like subtype (5.00%), Luminal A subtype (2.47%), Luminal B subtype (13.81%), and HER2 positive subtype (35.80%) (Fig. 2D). Moreover, a significant positive correlation was observed between the mRNA level of LRPPRC and the copy number of LRPPRC gene in TNBC (R Squired = 0.1632, *P* < 0.0001, Fig. 2E, F). Similar results were also obtained when using the hg38 as the as the reference genome (Supplemental file1: Figure S1 C).

In conclusion, the elevated expression of LRPPRC in TNBC was mainly caused by the reduced methylation level of cg14163061 at its promoter region and the elevated DNA copy number of LRPPRC gene.

LRPPRC promotes TNBC progression in vitro and in vivo

We then explored the functions of LRPPRC in TNBC progression, both in vitro and in vivo. SUM-159 and MDA-MB-468, two TNBC cells were transfected with the lentiviruses of Ctrl-shRNA as negative control or LRPPRC shRNA to attenuate LRPPRC expression (Fig. 3A and Supplemental file1: Figure S2A). The colony formation assay revealed that the knockdown of LRPPRC decreased the proliferative capacity of SUM-159 and MDA-MB-468 cells remarkably (51.71% inhibition in SUM-159; 32.75% inhibition in MDA-MB-468, Fig. 3B). The growth curve plotted with the Real Time Cellular Analysis (RTCA) results showed that the knockdown of LRPPRC slowed the cell proliferation rate in both two cell lines (Fig. 3C). In migration assay, the number of migrated cells attenuated substantially after LRPPRC knockdown in both SUM-159 (Ctrl-shRNA versus sh-LRPPRC-1, 38.13 versus 31.50, *P* = 0.0377) and MDA-MB-468 cells (Ctrl-shRNA versus sh-LRPPRC-1, 36.93 versus 13.07, *P* < 0.0001, Fig. 3D). In invasion assays, the number of invaded cells was also decreased by the LRPPRC depletion in SUM-159 (Ctrl-shRNA versus sh-LRPPRC-1, 29.27 versus 20.80, *P* < 0.0001) and MDA-MB-468 cells (Ctrl-shRNA versus sh-LRPPRC-1, 24.67 versus 6.40, *P* < 0.0001, Fig. 3E). To eliminate the off-target effects, we designed an additional shRNA sequence, which could also effectively reduce the expression level of LRPPRC and inhibit the malignant phenotype of cells, including proliferation, invasion, and migration (Supplemental file1: Figure S2 A-C, F).

To further confirm the functions of LRPPRC in TNBC-carcinogenesis in vivo, nude mice xenografts were established by subcutaneously injecting SUM-159 cells with and without LRPPRC knockdown. The growth curve of subcutaneous tumors showed that TNBC cells harbored a slower proliferation rate after the knockdown of LRPPRC. Subcutaneous tumors were harvested 42 days after cell injection. We then verified

the overexpression of LRPPRC in tumor samples using immunohistochemistry. 60.0% of control group samples were LRPPRC positive, which was significantly higher than that in LRPPRC knockdown group by sh-LRPPRC-1 (Fig. 3F). The statistics results showed that depletion of LRPPRC aroused a 71.5% inhibition in tumor size (*P* = 0.0078, Fig. 3G) and an 83.3% inhibition in tumor weight (*P* = 0.0062, Fig. 3H). Collectively, our results demonstrated that LRPPRC was necessary for TNBC progression, including cell proliferation, migration, and invasion in vitro and tumor growth in vivo.

LRPPRC promotes OXPHOS in TNBC cells

OXPHOS is the preferred metabolic pathway of TNBC cells, and the enhanced mitochondrial OXPHOS metabolism is a fundamental feature of TNBC. Published works proved the dependence of cancer cells on OXPHOS for energy production, cell survival, and chemosensitivity in vitro [20, 21] and tumor growth in vivo [8]. Our previous works have demonstrated that LRPPRC is one of the most important promoters of OXPHOS complex synthesis in lung cancer [13]. However, whether the overexpressed LRPPRC is also the driver oncoprotein responsible for OXPHOS activation in TNBC remains unclear. Therefore, we moved to investigate the roles of LRPPRC in OXPHOS synthesis in TNBC, especially in controlling the synthesis of the 13 proteins encoded by the mitochondrial genome. Real-time PCR showed a significant decrease of all the 13 mitochondrial genes at transcriptional level in SUM-159 cells, including ND1, ND2, ND3, ND4, ND4L, ND5, ND6 in complex I; CytB in complex III; COX-I, COX-II and COX-III in complex IV; and ATP6 and ATP8 in complex V (Fig. 4A and Supplemental file1: Figure S2 D). This declining tendency can be substantiated in more TNBC cell lines and LRPPRC knockdown with other shRNA sequence (Fig. 4B and Supplemental file1: Figure S2E).

The roles of LRPPRC in controlling the expression of OXPHOS complex subunits were further verified by western blot. A significant decrease in the protein level of mtDNA encoded COXII as well as Ubiquinol-Cytochrome C Reductase Core Protein 2 (UQCRC2) and NADH: Ubiquinone Oxidoreductase Subunit B8 (NDUFB8), two OXPHOS complex subunits that were affected by the expression of mitochondrial genome-encoded genes, was observed after LRPPRC knockdown (Fig. 4C and Supplemental file1: Figure S2F). We also reanalyzed the expression of LRPPRC and mitochondrial genome-encoded genes in TNBC samples from a public database. The correlation analysis results showed a robust positive correlation between LRPRPC mRNA level and that of ND1 (R = 0.49, *P* < 0.0001), ND2 (R = 0.47, *P* < 0.0001), CYTB (R = 0.20, *P* < 0.01), COX I

Xue *et al. Journal of Translational Medicine*   (2025) 23:372
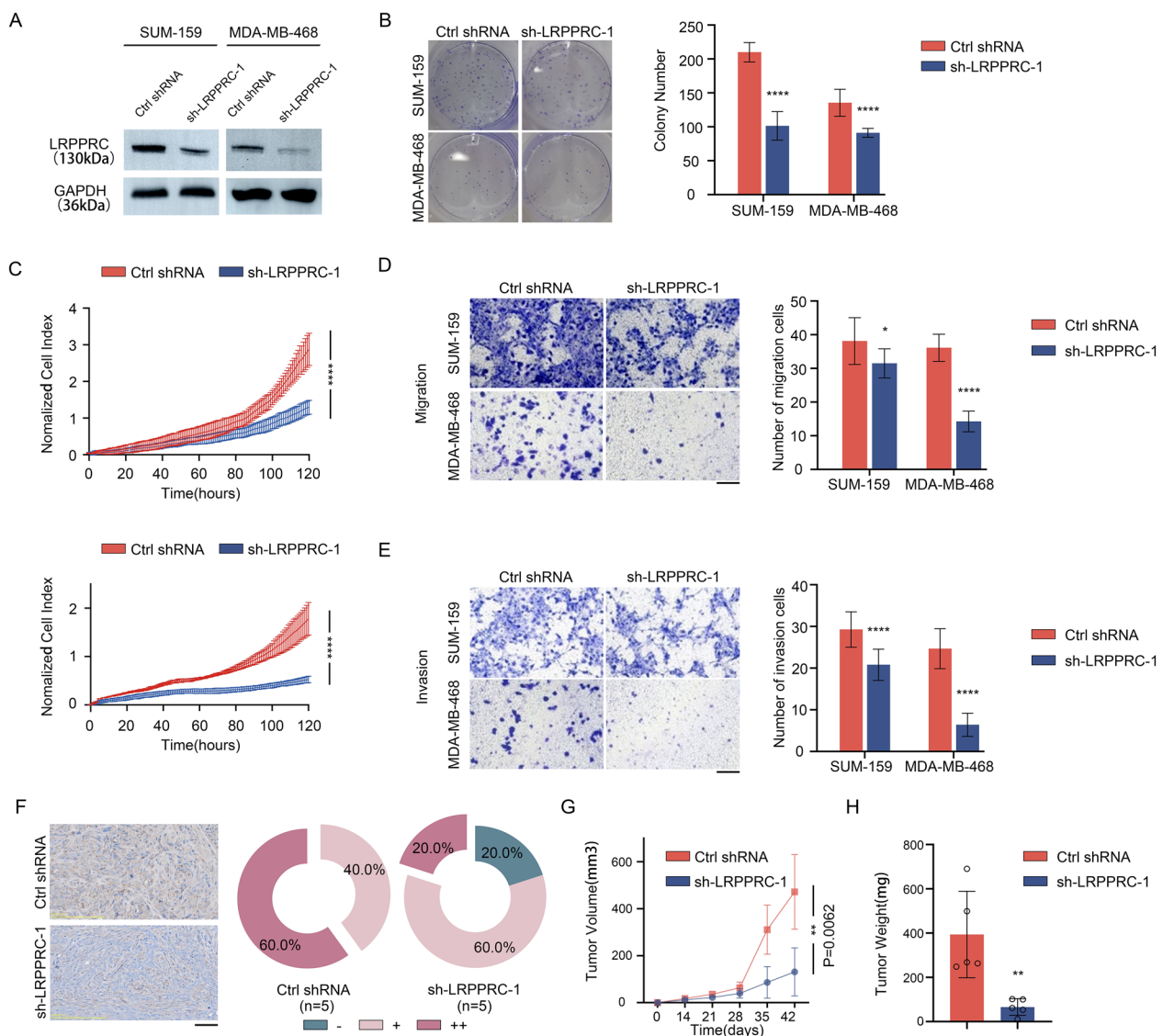
Page 8 of 15

Fig. 3 LRPPRC promotes cell proliferation, migration, and invasion. **A** Immunoblotting of LRPPRC protein in SUM-159 and MDA-MB-468 cells treated with lentivirus containing control shRNA or LRPPRC-specific shRNA. **B** Representative colony formation images of SUM-159 and MDA-MB-468 cell lines treated with lentivirus containing control shRNA or LRPPRC-specific shRNA. Colony formation data were summarized from independent experiments in triplicates and shown in histograms. Unpaired t-test was used. **C** Cell proliferation curves of SUM-159 (top) and MDA-MB-468 cells (bottom) treated with lentivirus containing control shRNA or LRPPRC-specific shRNA. Two-way ANOVA test was used. **D** Transwell assays to detect cell migration of SUM-159 and MDA-MB-468 cell lines treated with lentivirus containing control shRNA or LRPPRC-specific shRNA. Histogram analyses of migrated cell counts are shown. The number of migration cells was counted in ten random fields under a microscope. The scale bar is 50 μm. Unpaired t-test was used. **E** Transwell assays to detect cell invasion of SUM-159 and MDA-MB-468 cell lines treated with lentivirus containing control shRNA or LRPPRC-specific shRNA. Histogram analyses of migrated cell counts are shown. The invasive cells were counted in ten random fields under a microscope. The scale bar is 50 μm. Unpaired t-test was used. Subcutaneous injection of mice with 1×10^7 LRPPRC-shRNA-1 SUM-159 cells and negative control SUM-159 cells. Tumors were dissected at the end of the experiment. **F** Representative IHC images and quantification of IHC intensity of LRPPRC protein in subcutaneous TNBC tissues. Data were summarized from 5 independent mice in each group and shown in the pie graph. **G** Tumor volume of subcutaneous TNBC tissues with postinjection time. Two-way ANOVA test was used. **H** Tumor weight of subcutaneous TNBC tissues. Unpaired t-test was used

($R = 0.55$, $P < 0.0001$), and COX II ($R = 0.38$, $P < 0.0001$) in TNBC tumor samples (Fig. 4D). Taken together, LRPPRC

was necessary for the expression of mitochondrial

Xue *et al. Journal of Translational Medicine*   (2025) 23:372
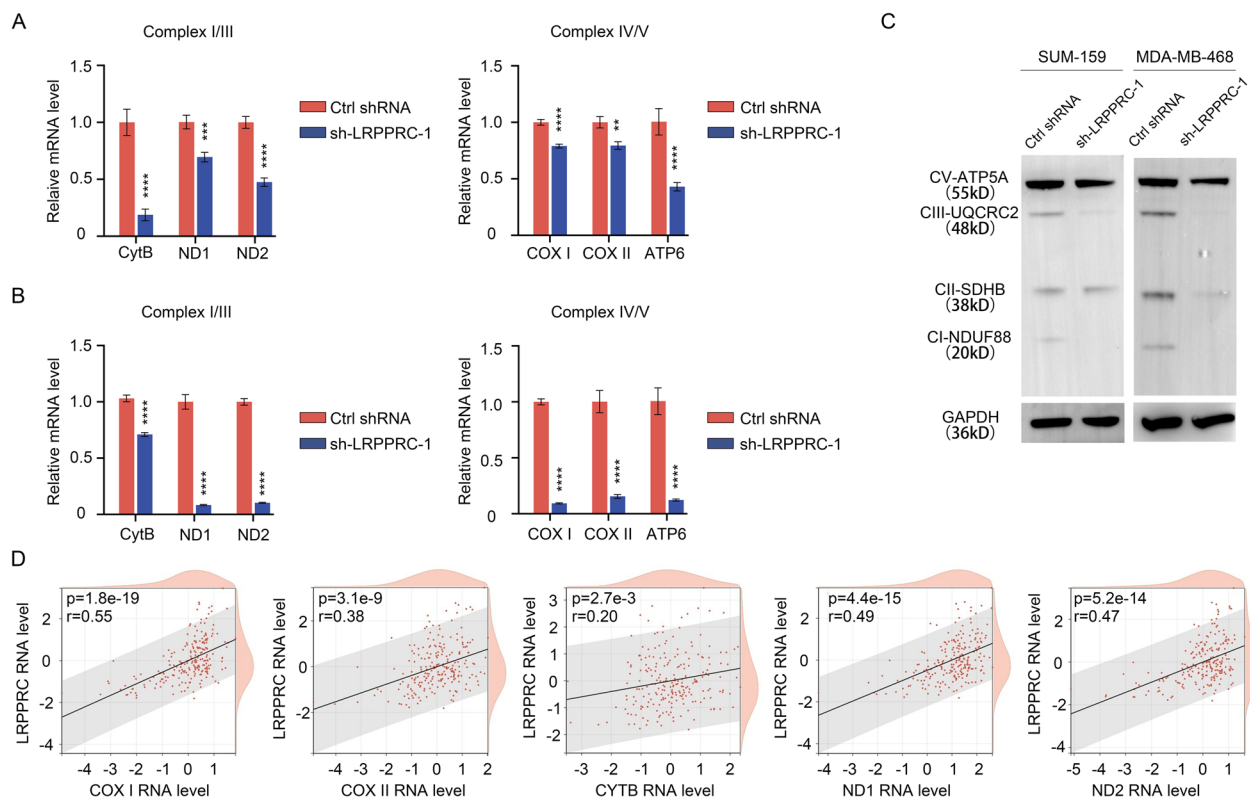
Page 9 of 15

Fig. 4 LRPPRC promotes OXPHOS in TNBC cells. **A** Quantification of the mRNA of complex I/III, and complex IV/V in SUM-159 cell treated with lentivirus containing control shRNA or LRPPRC-specific shRNA. The components of complex II are all encoded by the nuclear genome and are not shown in the figure. Unpaired t-test was used. **B** Quantification of the mRNA of complex IV, complex V, complex I, and III in MDA-MB-468 cell treated with lentivirus containing control shRNA or LRPPRC-specific shRNA. Unpaired t-test was used. **C** Immunoblotting of OXPHOS complex subunits in SUM-159 and MDA-MB-468 cells treated with lentivirus containing control shRNA or LRPPRC-specific shRNA. GAPDH, glyceraldehyde phosphate dehydrogenase. **D** Correlation analyses of LRPPRC expression and mitochondrial genome-encoded genes in TNBC samples by a public dataset (GSE142102). Simple linear regression test was used

genome-encoded OXPHOS-related genes, which was indispensable for the enhanced OXPHOS in TNBC.

GAA degrades LRPPRC protein and inhibits the synthesis of the OXPHOS complex in TNBC

In our previous work, we proved the traditional gynecological medicine gossypol acetate (GAA) could function as a LRPPRC-specific inhibitor by disrupting its interaction with mRNA and inducing LRPPRC degradation[13]. We then asked if GAA could be applied in TNBC to suppress the LRPPRC-mediated OXPHOS and tumor progression. Real-time PCR showed that the mRNA levels of all the 13 mitochondrial genome-encoded proteins we detected were reduced after GAA treatment in TNBC cell lines, especially COX-I and COX-II of complex IV and CytB of complex III. This inhibition exhibited a dose-dependent manner (Fig. 5A, B and Supplemental file1: Figure S3A, B). The protein levels of both LRPPRC itself and OXPHOS subunits were also detected by western blotting (Fig. 5C), which

demonstrated a significant decrease in the protein level of SDHB, and NDUFB8, similar to the tendency observed after LRPPRC knockdown.

We then tested the inhibition of mitochondrial oxygen consumption and ATP production after GAA administration and LRPPRC pharmacological inhibition. For this purpose, an oxygen consumption rate (OCR, an indication of oxygen consumption caused by OXPHOS) detecting assay was applied with both SUM-159 and MDA-MB-468 cell lines. In the OCR assay, three inhibitors against the OXPHOS process were introduced in order. The incubation of oligomycin can inhibit the function of complex V, suppress electron transfer, and lower OCR value. The addition of FCCP (Carbonyl cyanide 4-(trifluoromethoxy) phenylhydrazone), an uncoupling agent, will destroy the mitochondrial membrane potential. Therefore, the electron transportation and the OCR value will reach the maximum after FCCP incubating. At last, antimycin A and rotenone will inhibit the function of complex I,
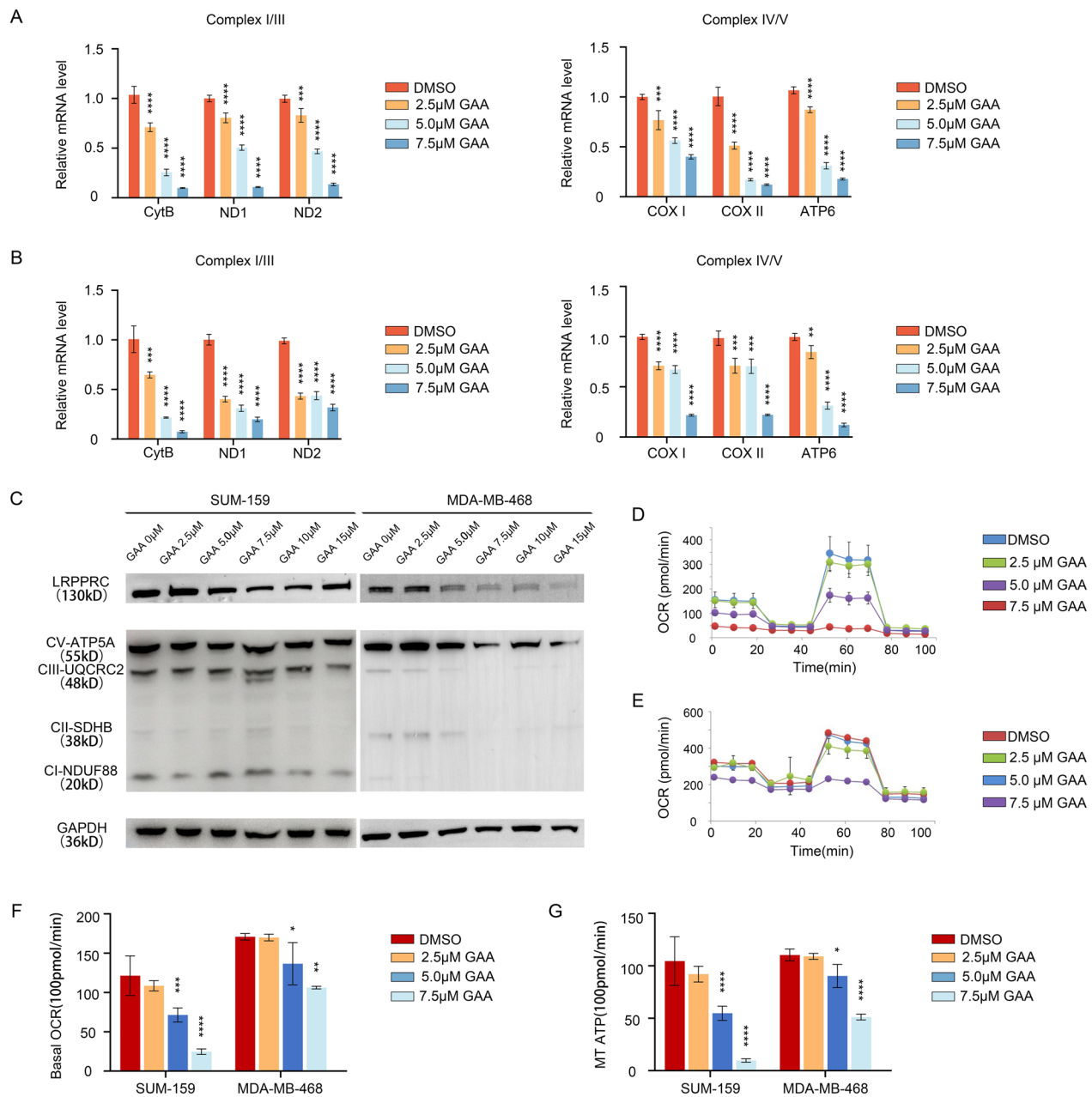
Xue *et al. Journal of Translational Medicine*   (2025) 23:372

Page 10 of 15

Fig. 5 GAA inhibits the synthesis of the OXPHOS complex. **A** Quantification of the mRNA of complex I/III, and complex IV/V mRNA in SUM-159 cells treated with GAA. The components of complex II are all encoded by the nuclear genome and are not shown in the figure. One-way ANOVA test was used. **B** Quantification of the mRNA of complex I/III, and complex IV/V mRNA in MDA-MB-468 cell treated with GAA. The components of complex II are all encoded by the nuclear genome and are not shown in the figure. One-way ANOVA test was used. **C** Immunoblotting of OXPHOS complex subunits in SUM-159 and MDA-MB-468 cells treated with GAA. **D** OCR analysis of SUM 159 cells treated with GAA. **E** OCR analysis of MDA-MB-468 cells treated with GAA. **F** Quantification of basal ORC of SUM-159 and MDA-MB-468 cells treated with GAA. One-way ANOVA test was used. **G** Quantification of MT ATP of SUM-159 and MDA-MB-468 cell lines treated with GAA. One-way ANOVA test was used

which can completely shut down the OXPHOS process and cause a sharp decline in OCR value. GAA-pretreated cells showed a slighter decrease in OCR after oligomycin addition, indicating an inhibited complex V function. Furthermore, the addition of FCCP could not increase the OCR of GAA-pretreated cells at all, suggesting that GAA-pretreated cells lost mitochondrial membrane potential (Fig. 5D, E). Further analysis proved that LRPPRC depletion by GAA resulted in a significant decrease in basal OCR, spare respiratory capacity, and

Xue *et al. Journal of Translational Medicine*   (2025) 23:372

Page 11 of 15

mitochondrial ATP production in both SUM-159 cells and MDA-MB-468 cells (Fig. 5F, G), indicating the inhibition of the function of OXPHOS complexes after GAA administration.

Our immunofluorescence results also supported the conclusion that GAA could affect the LRPPRC regulated mitochondrial function. More specifically, GAA treatment (0 μM, 2.5 μM, 5.0 μM) for 24 h not only reduced the membrane potential of mitochondria, but also decreased the number of mitochondria (Supplemental file1: Figure S4A,B).Therefore, the traditional gynecological medicine GAA could function as an LRPPRC inhibitor and suppress OXPHOS in TNBC.

GAA inhibits TNBC cell proliferation, migration, and invasion in vitro

To further assess the functions of GAA as a LRPPRC inhibitor for TNBC treatment, we treated two TNBC cell lines with GAA. The RTCA assays showed that GAA administration slowed TNBC cell proliferation in a dose-dependent manner and 5 μM GAA was enough to raise 80% inhibition in proliferation, for both SUM-159 and MDA-MB-468 cells (Fig. 6A). To complement the results from short-term treatments, we also performed long-term (14 days) colony-forming assays to determine if the inhibitory effects of GAA are sustained over time. At a concentration of 5 μM by GAA, the colony was inhibited in both SUM-159 and MDA-MB-468 cells (82.92% inhibition in SUM-159 and 25.96% inhibition in MDA-MB-468) , and 10 μM GAA was enough to suppress the colony completely (Fig. 6B). In Matrigel-free transwell assays, cell migration was significantly attenuated by GAA in SUM-159 cells (96.42% inhibition at 5 μM and 98.90% inhibition at 10 μM) and MDA-MB-468 cells (39.86% inhibition at 5 μM and 87.63% inhibition at 10 μM) (Fig. 6C). In Matrigel-coated invasion assays, cell invasion was also suppressed by GAA in SUM-159 cells (90.71% inhibition at 5 μM and 99.10% inhibition at 10 μM) and MDA-MB-468 cells (54.83% inhibition at 5 μM and 71.77% inhibition at 10 μM) (Fig. 6D). These data demonstrated the sensitive response to LRPPRC pharmacologic inhibition across different TNBC cell lines in vitro.

We also tortured the LRPPRC dependency of GAA-induced TNBC inhibition, reflecting the specificity of GAA. SUM-159 cells were treated with GAA before and after LRPPRC knockdown. Cell proliferation experiment based on RTCA system indicated GAA harbored a lower cell inhibition rate in LRPPRC knockdown SUM-159 cells than that of control SUM-159 cells (85.69% inhibition in control cells and 43.08% inhibition in LRPPRC knockdown cells, $P < 0.0001$, Fig. 6E, F). These results indicated the inhibitory effect of GAA against TNBC in vitro was largely dependent on LRPPRC expression.

GAA shows therapeutic prospects for TNBC in vivo

After clarifying the anti-tumor effect of the LRPPRC inhibitor, and its functions on the OXPHOS, we moved to test this strategy with the mice model. To improve the bioavailability and the degree of tumor enrichment, we prepared GAA-loaded bare mesoporous silica nanoparticles (MSNPs) [22]. MSNPs are biodegradable siliceous materials, the tumor enrichment and safety parameters of which have been well characterized in our previous works [23–25]. The MSNPs platform consists of a bare mesoporous silica core surrounded by PEG2000 and a lipid bilayer shell [22, 26, 27]. The mesoporous silica core can be loaded with GAA (Fig. 7A, B). The Nanoflow experiment showed the nanoparticles' average diameter was 127.3 nm (Supplemental file1: Figure S5A,B). This is a relatively ideal size, which is prone to the enhanced permeation, retention effect and tumor enrichment [27]. SUM-159 tumor-bearing mice were obtained by subcutaneous injection, and divided into two groups randomly. 150 μL GAA-loaded MSNPs (containing 360 μg GAA) were administrated by tail vein injection per 3 days. The MSNPs of the same silicon concentration as the GAA-loaded MSNPs were administered as the control group by tail vein injection. We found that the administration of GAA-loaded MSNPs led to an obvious tumor inhibition, reflected in a significantly slowed tumor proliferation rate. Subcutaneous tumors were harvested 40 days after cell injection. Immunohistochemistry staining demonstrated the LRPPRC protein level in GAA treated mice was suppressed (Fig. 7C). The tumor volume and tumor weight of the GAA treatment group were reduced by 80% and 69.76% respectively (Fig. 7D, E). Therefore, LRPPRC inhibition by GAA showed a good anti-tumor ability in vivo. These results indicated that using small molecule LRPPRC inhibitor GAA could be a new treatment strategy for TNBC.

Discussion

In this study, we discovered that the LRPPRC served as a distinct biomarker for TNBC and investigated the underlying molecular mechanisms responsible for the elevated expression of LRPPRC in TNBC. Furthermore, the impact of LRPPRC on the onset and progression of TNBC was examined both in vitro and in vivo. Ultimately, we showcased the potential therapeutic application of a LRPPRC-specific small molecule inhibitor, the classic gynecological medication GAA, in the treatment of TNBC. Overall, this work not only identified a therapeutic target for TNBC but also proposed an alternative intervention approach.
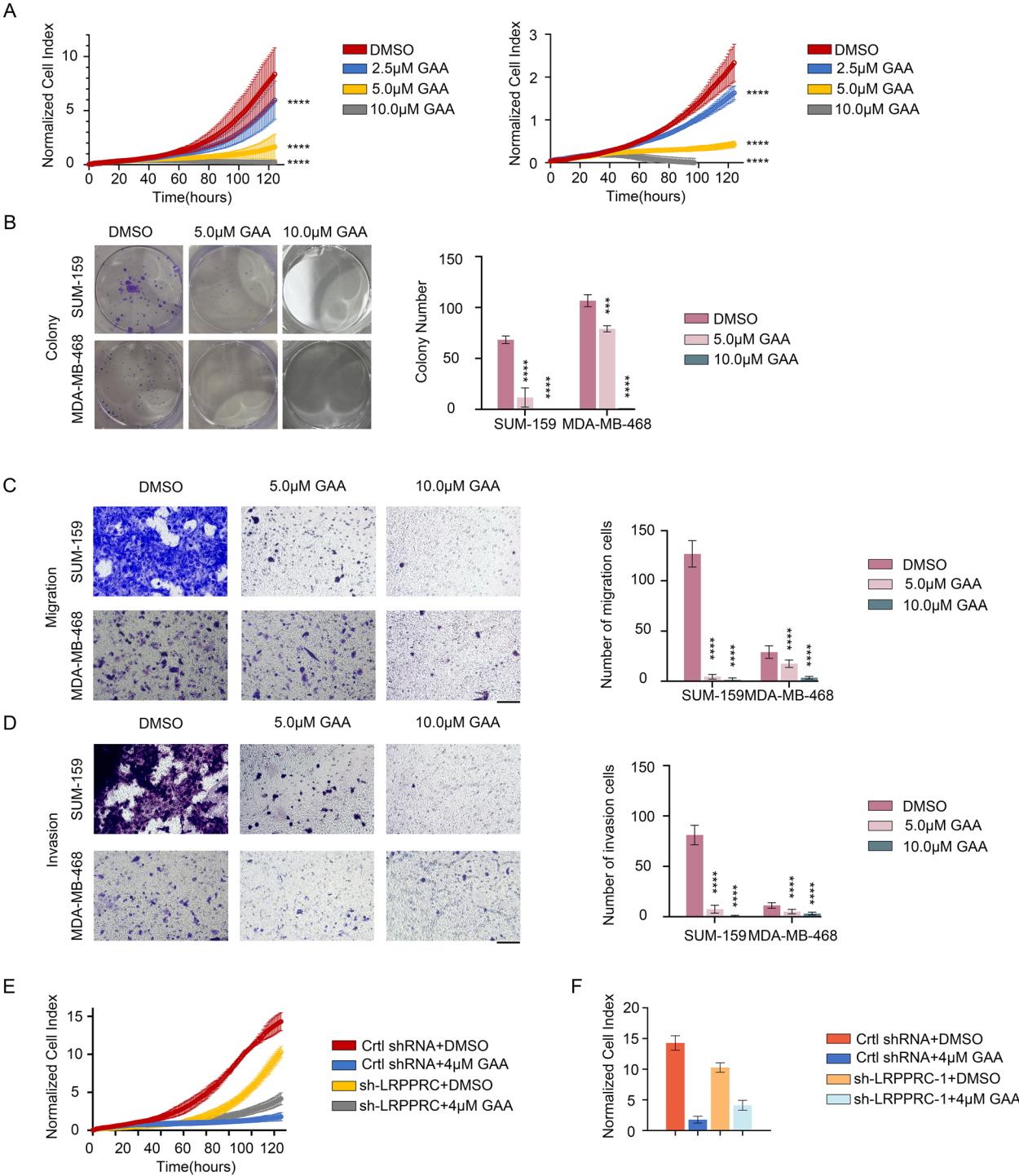
Fig. 6 GAA targeting LRPPRC inhibits cell proliferation, migration, and invasion in TNBC cells. **A** Cell proliferation curves of SUM-159 cells (left) and MDA-MB-468 cells (right) treated with GAA for 120 h. Two-way ANOVA test was used. **B** Representative colony formation images of SUM-159 and MDA-MB-468 cells after being treated by GAA. Colony formation data were summarized from independent experiments in triplicates and shown in histograms. One-way ANOVA test was used. **C** Transwell assays to detect cell migration of SUM-159 and MDA-MB-468 cell lines treated with GAA. Histogram analyses of migrated cell counts are shown. The number of migration cells was counted in ten random fields under a microscope. One-way ANOVA test was used. **D** Transwell assays to detect cell invasion of SUM-159 and MDA-MB-468 cell lines treated with GAA. Histogram analyses of migrated cell counts are shown. The invasive cells were counted in ten random fields under a microscope. One-way ANOVA test was used. **E** Cell proliferation of SUM-159 cells (before and after LRPPRC knockdown) treated with GAA 120 h. Unpaired t-test was used. **F** Quantification of normalized cell index of SUM-159 and MDA-MB-468 cells treated with GAA for 120 h
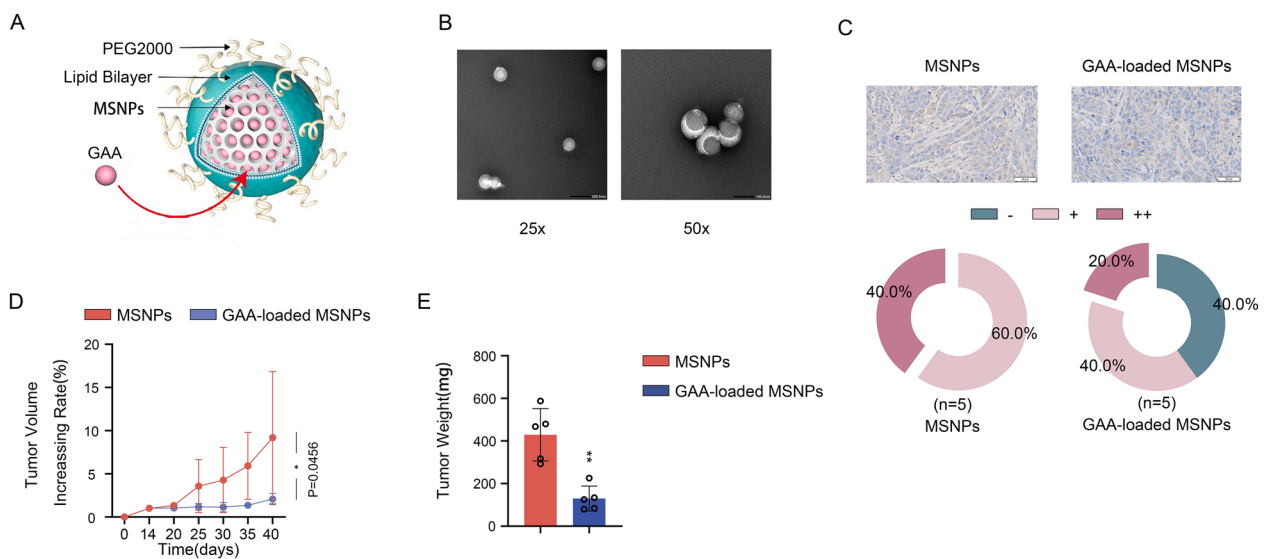
Xue *et al. Journal of Translational Medicine*   (2025) 23:372

Page 13 of 15

Fig. 7 Prospects of GAA as a therapeutic agent for TNBC. **A** The MSNPs platform consists of a bare mesoporous silica core surrounded by PEG2000 and a lipid bilayer shell. The mesoporous silica core can be loaded with GAA. **B** TEM images of GAA MSNPs. **C** Representative IHC images and quantification of IHC intensity of LRPPRC protein in subcutaneous TNBC tissues treated with GAA MSNPs. Data were summarized from independent experiments in triplicates and shown in the pie graph. **D** Tumor volume of subcutaneous TNBC tissues with postinjection time treated with GAA MSNPs. Two-way ANOVA test was used. **H** Tumor weight of subcutaneous TNBC tissues treated with GAA MSNPs. Unpaired t-test was used

TNBC is a highly aggressive tumor, with extremely limited treatment options. Recent studies have shown that the LRPPRC is overexpressed in TNBC [28, 29]. However, the reason for the high expression of LRPPRC in TNBC has not been explained yet, and the molecular mechanism of LRPPRC promoting the progress of TNBC remains unclear. Our work found that the high expression of LRPPRC in TNBC was driven by specific DNA promoter methylation abnormality and copy number amplification. Meanwhile, we demonstrated that LRPPRC promoted the progression of TNBC by enhancing mitochondrial oxidative phosphorylation. Therefore, our work provided new experimental evidence for the diagnostic markers of TNBC and an important reference for understanding the molecular mechanism in the occurrence and development of TNBC, especially the mechanism of metabolic abnormalities.

Numerous studies have verified the enhanced mitochondrial oxidative phosphorylation metabolism in TNBC. The robust oxidative phosphorylation confers TNBC cells increased resistance to chemotherapy and a more potent ability to metastasize. The oxidative phosphorylation complex is co-encoded by both the mitochondrial and nuclear genomes. Prior works have shown that RB1, a gene that is commonly mutated and inactivated, provides a comprehensive explanation for the up-regulation of the oxidative phosphorylation complex encoded by the nuclear genome in TNBC. Nevertheless,

how TNBC upregulates the expression of oxidative phosphorylation subunits encoded by mitochondrial genes remains unclear. From this standpoint, we have discovered that TNBC particularly augmented the expression of LRPPRC protein by modifying the DNA copy number and the promoter methylation degree of LRPPRC gene. The LRPPRC protein, which is found in the mitochondria, improves the durability and translation efficiency of RNA encoded by mitochondrial genes. As a result, it boosts the production of oxidative phosphorylation complex subunits encoded by mitochondrial genes. The findings of our research have important insight for elucidating the metabolic characteristics of TNBC.

The inhibition of mitochondrial OXPHOS to impede the progression of TNBC has emerged as a research hotspot. Several medicines, including metformin and IACS-010759, are undergoing clinical tests [30]. Nevertheless, all these medications directly suppress the electron transfer activity of oxidative phosphorylation complex I. As normal tissue cells also depend on oxidative phosphorylation for energy production, they are unable to differentiate normal tissue cells and cancer cells. Targeting LRPPRC to decrease oxidative phosphorylation can effectively and specifically suppress TNBC from several approaches. LRPPRC is specificity upregulated in TNBC cells, indicating the inhibitory effect of GAA could be more restricted in

cancer cells. On the other hand, LRPPRC inhibitors do not directly impede the functioning of pre-existing mitochondrial oxidative phosphorylation complexes but rather hinder the synthesis of new mitochondrial oxidative phosphorylation complexes. Normal tissue cells with slow proliferation exhibit a sluggish updating of the mitochondrial oxidative phosphorylation complex and are relatively resistant to LRPPRC inhibitors. The rapid growth of cancer cells necessitates the swift production of mitochondrial oxidative phosphorylation complexes to fulfill their proliferation requirements. These characteristics also govern their vulnerability to LRPPRC inhibitors. However, we noticed that different TNBC cell lines showed different sensitivity against GAA. This may be due to two cells having different levels of LRPRPC expression, as reported in our previous work [31]. Investigating the mechanism that governs GAA sensitivity will have significant ramifications for future precision medicine. Therefore, our research offers valuable guidance for the advancement of specific techniques to suppress oxidative phosphorylation in cancer cells.

At last, our current work arouses research interests for further investigation, such as searching for other small molecule inhibitors that have better efficacy than GAA and exploring other molecular mechanisms response for high LRPPRC expression level in tumor progression. We will continue our efforts in this area.

Abbreviations

TNBC	Triple-negative breast cancer
OXPHOS	Oxidative phosphorylation
GAA	Gossypol acetate
LRPPRC	Leucine-rich pentatricopeptide repeat containing protein
IHC	Immunohistochemistry
WB	Western-blot
OCR	Oxygen consumption rate

Supplementary Information

The online version contains supplementary material available at https://doi.org/10.1186/s12967-024-05946-6.

> Additional file 1
>
> Additional file 2

Author contributions
Qiqi Xue: carried out WB, PCR experiments, drug sensitivity test, performed cell culture; wrote original draft. Wenxi Wang: carried out IHC experiments, statistical analysis, animal experiments, wrote original draft. Jie Liu: performed cell phenotype experiments; Dachi Wang: performed confocal imaging experiments; Tianyu Zhang: characterized MSNPs; Tingting Shen: performed cell culture; Xiangsheng Liu: provided MSNPs; Xiaojia Wang: performed statistical analysis; Xiying Shao: supervised the project; Wei Zhou: designed and supervised the project; Xiaohong Fang: designed and supervised the project; wrote the paper.

Availability of data and materials
All data generated or analyzed during this study are included in the manuscript and its additional information files.

Declarations

Ethics approval and consent to participate
All samples were collected with informed consent and ethical approval was acquired from the Ethics Committee of Zhejiang Cancer Hospital (ZJCH).

Consent for publication
All authors agreed on the manuscript.

Competing interests
The authors declare that they have no competing interests.

Author details
[1]Hangzhou Institute for Advanced Study, University of Chinese Academy of Sciences, Hangzhou 310024, China. [2]Hangzhou Institute of Medicine, Chinese Academy of Sciences, Hangzhou 310018, Zhejiang, China. [3]Institute of Chemistry, Chinese Academy of Sciences, Beijing 100190, China. [4]Zhejiang Cancer Hospital, Hangzhou 310022, China.

References
1. Sung H, et al. Global Cancer Statistics 2020: GLOBOCAN Estimates of Incidence and Mortality Worldwide for 36 Cancers in 185 Countries. CA Cancer J Clin. 2021;71(3):209–49.
2. Goldhirsch A, et al. Personalizing the treatment of women with early breast cancer: highlights of the St Gallen International Expert Consensus on the Primary Therapy of Early Breast Cancer 2013. Ann Oncol. 2013;24(9):2206–23.
3. Waks AG, Winer EP. Breast Cancer Treatment. JAMA. 2019;321(3):316.
4. Wolff AC, et al. Recommendations for human epidermal growth factor receptor 2 testing in breast cancer: American Society of Clinical Oncology/College of American Pathologists clinical practice guideline update. J Clin Oncol. 2013;31(31):3997–4013.
5. Yin L, et al. Triple-negative breast cancer molecular subtyping and treatment progress. Breast Cancer Res. 2020;22(1):61.
6. Galli A, et al. PFKP is transcriptionally repressed by BRCA1/ZBRK1 and predicts prognosis in breast cancer. PLoS ONE. 2020;15(5):e0233750.
7. Knudsen ES, et al. RB loss contributes to aggressive tumor phenotypes in MYC-driven triple negative breast cancer. Cell Cycle. 2015;14(1):109–22.
8. Wu Q, et al. GLUT1 inhibition blocks growth of RB1-positive triple negative breast cancer. Nat Commun. 2020;11(1):4205.
9. Hernandez-Resendiz I, et al. Dual regulation of energy metabolism by p53 in human cervix and breast cancer cells. Biochim Biophys Acta. 2015;1853(12):3266–78.
10. Liu L, et al. LRP130 protein remodels mitochondria and stimulates fatty acid oxidation. J Biol Chem. 2011;286(48):41253–64.
11. Akie TE, et al. OXPHOS-mediated induction of NAD+ promotes complete oxidation of fatty acids and interdicts non-alcoholic fatty liver disease. PLoS ONE. 2015;10(5): e0125617.
12. Lei S, et al. Increased hepatic fatty acids uptake and oxidation by LRPPRC-driven oxidative phosphorylation reduces blood lipid levels. Front Physiol. 2016;7:270.
13. Zhou W, et al. The RNA-binding protein LRPPRC promotes resistance to CDK4/6 inhibition in lung cancer. Nat Commun. 2023; 14(1).

Xue *et al. Journal of Translational Medicine*   (2025) 23:372

Page 15 of 15

14. Yang Y, et al. Targeting the miR-34a/LRPPRC/MDR1 axis collapse the chemoresistance in P53 inactive colorectal cancer. Cell Death Differ. 2022;29(11):2177–89.
15. Wang W, et al. Practical strategy to 1,1´-dideoxygossypol derivatives from gossypol and its antitumor activities. ACS Omega. 2022;7(26):22938–43.
16. Cao Y, et al. Intratumoural microbiota: a new frontier in cancer development and therapy. Signal Transduction Targeted Therapy. 2024; 9(1).
17. Chandrashekar DS, et al. UALCAN: a portal for facilitating tumor subgroup gene expression and survival analyses. Neoplasia. 2017;19(8):649–58.
18. Koch A, et al. MEXPRESS: visualizing expression, DNA methylation and clinical TCGA data. BMC Genomics. 2015;16(1):636.
19. Koch A, et al. MEXPRESS update 2019. Nucleic Acids Res. 2019;47(W1):W561–5.
20. Molina JR, et al. An inhibitor of oxidative phosphorylation exploits cancer vulnerability. Nat Med. 2018;24(7):1036–46.
21. Weinberg F, et al. Mitochondrial metabolism and ROS generation are essential for Kras-mediated tumorigenicity. Proc Natl Acad Sci. 2010;107(19):8788–93.
22. Liu X, et al. Irinotecan delivery by lipid-coated mesoporous silica nanoparticles shows improved efficacy and safety over liposomes for pancreatic cancer. ACS Nano. 2016;10(2):2702–15.
23. Lu J, et al. Biocompatibility, biodistribution, and drug-delivery efficiency of mesoporous silica nanoparticles for cancer therapy in animals. Small. 2010;6(16):1794–805.
24. Xinglu Huang LL, Liu T, Hao N, Liu H, Chen D, Tang F. The shape effect of mesoporous silica nanoparticles on biodistribution, clearance, and biocompatibility in vivo. ACS Nano. 2011;5:5390.
25. Liu T, et al. Single and repeated dose toxicity of mesoporous hollow silica nanoparticles in intravenously exposed mice. Biomaterials. 2011;32(6):1657–68.
26. Liu X, et al. Improved efficacy and reduced toxicity using a custom-designed irinotecan-delivering silicasome for orthotopic colon cancer. ACS Nano. 2018;13(1):38–53.
27. Liu X, et al. Tumor-penetrating peptide enhances transcytosis of silicasome-based chemotherapy for pancreatic cancer. J Clin Investig. 2017;127(5):2007–18.
28. Yu Y, et al. LRPPRC promotes glycolysis by stabilising LDHA mRNA and its knockdown plus glutamine inhibitor induces synthetic lethality via m6A modification in triple-negative breast cancer. Clin Transl Med. 2024; 14(2).
29. Lv S, et al. Cyclopropenone, cyclopropeniminium ion, and cyclopropenethione as novel electrophilic warheads for potential target discovery of triple-negative breast cancer. J Med Chem. 2023;66(4):2851–64.
30. Evans KW, et al. Oxidative phosphorylation is a metabolic vulnerability in chemotherapy-resistant triple-negative breast cancer. Cancer Res. 2021;81(21):5572–81.
31. Zhou W, et al. Proteasome-independent protein knockdown by small-molecule inhibitor for the undruggable lung adenocarcinoma. J Am Chem Soc. 2019;141(46):18492–9.

Publisher's Note

Springer Nature remains neutral with regard to jurisdictional claims in published maps and institutional affiliations.